Comparison between simulation and experimental results of a PSA process for production of H_2 used in fuel cells

Amna Abdeljaoued [#1], Frederico Relvas [*2], Adélio Mendes[*3], Mohamed Hachemi Chahbani[#4]

[#] UR11ES80— Applied Thermodynamics Research Unit, Department of Chemical Engineering, National School of Engineers of Gabes, Tunisia.

[*]LEPAE—Laboratory for Process, Environmental and Energy Engineering, Department of Chemical Engineering, Faculty of Engineering, Porto University, Portugal

[1]amnaamouna2009@hotmail.com
[4]chahbani.med_hachemi@yahoo.com
[2]frelvas@fe.up.pt
[3]mendes@fe.up.pt

Abstract*— In recent years, considerable effort has been made to develop technologies for harvesting energy from renewable sources. Hydrogen can be used in fuel cells to produce electricity very efficiently and cleanly. Among the various processes proposed, steam reforming of ethanol for hydrogen production is very attractive. In the steam reforming reaction, in addition to H_2 and CO_2, significant amounts of CO and CH_4 are also formed due to side reactions. Prior to design a Pressure Swing Adsorption (PSA) unit aiming at producing H_2 with very small amounts of CO, it is essential to experimentally determine the adsorption equilibrium isotherms and mass transfer kinetics data of the multicomponent system (H_2, CH4, CO_2, CO). A theoretical twelve- step four-column PSA model has been developed for studying impurity removal from steam reforming of ethanol for producing ultra-pure hydrogen. The model* **which is implemented in Aspen Adsorption** *was validated by experimental data on a commercial activated carbon. Breakthrough curves, the bed temperature distribution and PSA results shows good agreement with experiments.

***Keywords*— H2 production, breakthrough curves, adsorption equilibrium isotherms, simulation, PSA process, experimental validation**

I. INTRODUCTION

The desire to reduce greenhouse gas emissions and limited resources in supplying fossil fuels have led to demands for diversifying energy resources as a priority. A considerable effort has been expended in developing technologies for using renewable energy sources. Hydrogen can be used in fuel cells to produce electricity very efficiently and cleanly. Among the various processes proposed, steam reforming of ethanol for hydrogen production is very attractive.

A further advantage is that, supported by appropriate storage technologies, hydrogen can be utilized for domestic consumption as it can be safely transported through conventional means [1–2].

A number of experimental and theoretical studies have been carried out to investigate hydrogen separation from SMR off-gas, oven coke gas, or refinery fuel gas by PSA process using single/layered-bed configuration [3–4].

In the steam reforming reaction, in addition to H_2 and CO_2, significant amounts of CO and CH_4 are also formed due to side reactions. For use in fuel cells, the CO content has to be reduced to low values because it poisons the platinum catalyst present in the Membrane Electrode Assemblies (MEA) of Polymer Electrolyte Membrane Fuel Cell (PEMFC).

Pressure swing adsorption (PSA) units are commonly used in hydrogen purification from reforming gas [3-5]. The present work focuses on the separation of hydrogen from a four component mixture ($H2/CO_2/CH_4/CO$) using a twelve steps, four-column pressure swing adsorption.

In the PSA simulation a 99.9913 % hydrogen purity stream (with 84.39 ppm of CO, 0.17 ppm of CO2 and 0.9 ppm of CH4 contamination) was obtained with a hydrogen recovery of 75.5 %.

As a consequence, to study hydrogen purification through a PSA process, it is necessary to determine the adsorption equilibria and kinetics data of the multicomponent systems [6]. A gas mixture (1% CO, 25% CO_2, 5% CH_4 and 69% H_2) that has the same composition as the reforming gas was prepared. A commercial activated carbon was selected as adsorbent for this study.

In the present work, a series of experimental data of multicomponent mixture including adsorption isotherms, breakthrough curves and PSA is provided. Further, a mathematical model that includes mass, energy and momentum balances was employed to elucidate the dynamic behaviours and separation performance of the adsorption bed and optimization purposes.

II. EXPERIMENTAL SECTION

II.1 MATERIAL AND METHODS

II.1.1Material

A four-component hydrogen mixture gas (CO: CO_2:CH_4:H_2 = 1:25:5:69 mol %) that has the same composition as the reforming gas was synthesized. A commercial activated carbon was selected for the study.

Helium pycnometry was used to determine the real density of the adsorbent while Mercury porosimetry was used to determine apparent density. The physical properties of the adsorbent are listed in Table 1.

Property	**Value**
Geometry	cylindrical
Real density *[g·cm^3]* – He picnometry	1.969
Average particle diameter, *[mm]*	1.202
Apparent density [*g·cm^3]* - Hg porosimetry	0.944

Table 1: Physical properties of the adsorbent.

II.1.2Methods

II.1.2.1 Equilibrium isotherms

The determination of carbon monoxide, carbon dioxide, methane and hydrogen equilibrium isotherms was conducted using the volumetric method. This technique is based on pressure variation of the relevant gas after an expansion. Assuming the ideal gas behaviour and knowing the pressure drop, it is possible to determine the gas quantity adsorbed. The volumetric method apparatus is described elsewhere [7].

II.1.2.2 Breakthrough curves

To measure the adsorption data of multicomponent mixtures, an experimental setup composed of one column filled with a commercial activated carbon, at the entrance and the exit of this column we insert a thermocouple, two pressure transducers (Druck PMP 4010, with pressure range variation from 0 to 7 bars (±0.08 % FS), two mass flow meter controllers, one for the feed flow (Bronkhorst El-flow, 100 $mL_{PTN}min^{-1}$ and a range of 0-2 LPTN min^{-1}, ± 0.5 % Rd plus ±0.1 % FS) and the other for exit flow (Bronkhorst El-flow, 010 L_{PTN} min^{-1} (±0.5 % Rd plus (±0.1 % FS), and a vacuum pump (Ilmvac, MPC201T) for the desorption step. To ensure an isothermal operation the setup is placed inside a thermostatic chamber .The composition of the gas of the outlet flow were determined using mass spectrometer. The apparatus is described elsewhere [8]. The breakthrough experimental setup is shown in figure 1.

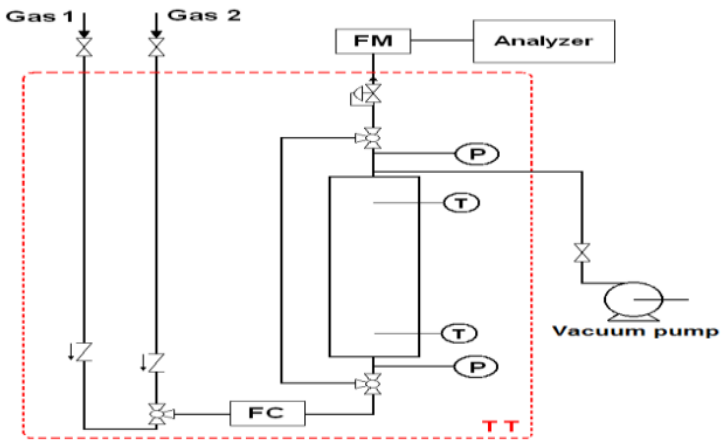

Figure 1: Experimental setup for measurement of breakthrough curves.

The bed characteristics are summarized in Table 2.

Adsorption bed	
Bed length, L *[cm]*	34
Inside radius, r_i *[cm]*	3.2
Outside radius, r_o, *[cm]*	3.5
Material of wall [-]	Stainless steel
Heat capacity of wall, Cp_w [J/kg K]	502
Inter- particle voidage	0.385
Intra-particle voidage	0.521
Thermal conductivity of the wall, K_w [J/m K s]	16.3

Table 2: Characteristics of the adsorption bed.

II.1.2.3 PSA unit

The lab-scale of the pilot PSA system is shown in Figure 2.

To measure the PSA data of multicomponent mixtures, a PSA unit composed of four columns which have an inner diameter of 2.2 cm and a length of 27.5cm. They were filled with ~89.73 g of a commercial activated carbon.

Two thermocouples type K were installed at positions 2.5 and 25 cm from the feed end to measure temperature variations inside the adsorption bed, four pressure transducers (Druck, PMP 4010, 0 – 10 bar) were located in each column to measure the pressure history during operation.

The feed section was equipped with four Bronkhorst mass flow controllers' series F201C and F201CV, which are connected to methane, carbon monoxide cylinders and to the carbon dioxide and hydrogen gas grid of the laboratory.

Figure 2: the pilot PSA system.

A 3 L buffer tank was used as a feed storage tank to prepare a synthetic reformate gas mixture with a composition of 73 % of H2, 25 % of CO2, 1 % of CH4 and 1 % of CO, to avoid pressure fluctuations.

The system was automatically operated by a personal computer that was interfaced with Lab View software with a built-in control program.

Solenoid valves were activated according to a process time schedule. Eight solenoid Asco SCE37CA056nv were placed in the feed and off-gas side (4 for each side), SC G325B031were used to control the equalization steps and SC G325B031 were placed in product and purge lines positions. To prevent dispensable reverse flow Some Swagelok poppet check valves, SS-2C-1/3 were installed at the proper positions. the amounts of gas flow into the PSA system was monitored with a mass flow meter (Bronkhorst High-tech, El Flow F-112AC, 0 – 20 dm3·min-1) , the purge flow rate was measured using a mass flow meter (Bronkhorst High-tech, El Flow F-111C, 0 – 2 dm3·min-1) and the product flow rate was controlled using a mass flow controller (Bronkhorst High-tech, El-Flow F-201CV, 0 – 10 dm3·min-1). The purge flow rate was regulated using a needle valve.

Product samples were passed through the sampling line that was connected to the product tank and were analyzed using a gas chromatograph DANI GC1000.Carbon monoxide composition was measured by a gas analyzer Signal Instruments 7100FM equipped with two sensors for different ranges, from 0.1 ppm up to 5000 ppm. Carbon dioxide was analyzed by a Thermo Scientific Analyzer model 410i. All of the measured data were monitored and saved on the interfaced computer through and AD converter.

III. MATHEMATICAL MODEL

III.1 Model assumptions

The dynamic behavior of the adsorption bed and the PSA process is described by a mathematical model which couples mass, momentum and energy balances over a packed bed. The following assumptions were adopted:

- The ideal gas behavior.
- The multicomponent adsorption equilibrium is represented by the dual site Langmuir isotherm.
- There are no radial variations in temperature, pressure, concentration, or velocity.
- The adsorption rate is approximated by a linear driving force (LDF).
- The pressure drop through the bed during adsorption and purge steps is described by Ergun's Equation.
- Non-isothermal energy balance with gas and solid conduction.

III.2 Model equations

The mass balance equations for each component and for the total mass of mixture are presented by equations (1) and (2), respectively.

$$u\frac{\partial c_i}{\partial z}+c_i\frac{\partial u}{\partial z}+\rho_p\frac{(1-\varepsilon_{bed})}{\varepsilon_{bed}}\frac{\partial q}{\partial t}=0 \qquad (1)$$

$$c\frac{\partial u}{\partial z}+\frac{\partial c}{\partial T}+\rho_p\frac{(1-\varepsilon_{bed})}{\varepsilon_{bed}}\sum_{i=1}^{n}\frac{\partial q_i}{\partial T}=0 \qquad (2)$$

Where u is the gas interstitial velocity, c_i is the gas concentration of component i, ρ_p is the particle density, ε_{bed} is the bed porosity, q_i is the adsorbed concentration of component i.

The adsorption rate is given by the linear driving force (LDF) model:

$$\frac{\partial q_i}{\partial t}=k_i(q_i^*-q_i) \qquad (3)$$

Where k_i is the mass-transfer coefficient; q_i^* is the loading of component i , and can be calculated by the dual-site Langmuir isotherm model:

$$q_i^*=\frac{q_{m1i}B_{1i}P_i}{1+\sum_{i=1}^{n}B_{1i}P_i}+\frac{q_{m2i}B_{2i}P_i}{1+\sum_{i=1}^{n}B_{2i}P_i} \qquad (4)$$

$$B_{1i}=k_{3i}\exp(\frac{k_{2i}}{T}) \qquad (5)$$

$$B_{2i}=k_{5i}\exp(\frac{k_{6i}}{T}) \qquad (6)$$

$$k_{1i}=k_{3i}q_{m1i} \qquad (7)$$

$$k_{4i}=k_{5i}q_{m2i} \qquad (8)$$

$$k_{2i}=\frac{\Delta H_{1ads}}{R} \qquad (9)$$

$$k_{6i}=\frac{\Delta H_{2ads}}{R} \qquad (10)$$

For the simulation, it was assumed that the heat of adsorption on the first and second sites are equal: $\Delta H_{1,ads}=\Delta H_{2,ads}$.

The Ergun equation was used as a simplified momentum balance equation to calculate the pressure drop along the bed.

$$-\frac{\partial p}{\partial z}=150\frac{\mu V_z(1-\varepsilon_{bed})^2}{{d_p}^2\varepsilon^2_{bed}}+1.75\frac{\rho_g {V_z}^2(1-\varepsilon_{bed})^2}{d_p\varepsilon_{bed}}\frac{1}{n} \qquad (11)$$

V_z is velocity.

III.3 PSA simulation

The models presented in Section 2 were applied for the simulation of a four- column PSA process with twelve elementary steps. The cycle sequence considered is schematically represented in Figure 3 as follows:
Adsorption, AD
First Depressurising Pressure Equalization, FDPE
Providing Purge, PP
Second Depressurising Pressure Equalization, SDPE
Blowdown, BD
Purge, PR
First pressurising Pressure Equalization, FPPE
Second pressurising Pressure Equalization, SPPE
Idle step all valves are closed
Pressurisation, PR

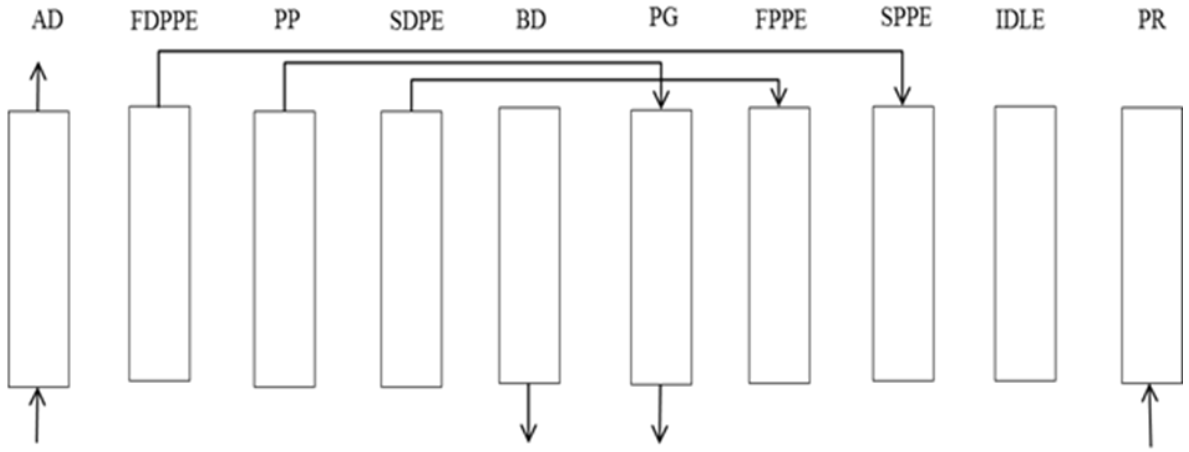

Figure 3: schematic diagram of the cycles sequences used in the PSA simulation.

Table 3 show the step configuration where the providing purge step is located between the two DPE steps has a clear advantage over a cycle where the providing purge step follows the two DPE steps in that it can increase the purge flow rate to a greater extent since the providing purge step can start at a higher pressure**[9].**

Step	1	2	3	4	5	6	7	8	9	10	11	12
Bed 1	AD			FDPE	PP	SDPE	BD	PG	FPPE	SPPE	IDLE	PR
Bed 2	SPPE	IDLE	PR	AD			FDPE	PP	SPPE	BD	PG	FPPE
Bed 3	BD	PG	FPPE	SPPE	IDLE	PR	AD			FDPE	PP	SDPE
Bed 4	FDPE	PP	SDPE	BD	PG	FPPE	SPPE	IDLE	PR	AD		
Time(s)	1.5	97	1.5	1.5	97	1.5	1.5	97	1.5	1.5	97	1.5

Table 3: Cyclic sequences of four-bed PSA process.

During the first pressurizing equalization step a considerable amount of hydrogen is released from the column, which used for purging the column which is in the purge step.

The boundary conditions for the gas phase concentrations and the temperature are given in table 4.

Adsorption bed inlet (Z=0)	Adsorption bed outlet (Z=L)
Adsorption (AD)	
$-\xi_b D_Z \frac{\partial C_j(0)}{\partial Z} = u(0)(C_j^{Feed} - C_j(0))$	$\frac{\partial C_j(L)}{\partial Z} = 0$
$-\xi_b K_Z \frac{\partial T(0)}{\partial Z} = u(0)\rho_g(0)C_{pg}(0)(T^{Feed} - T(0))$	$\frac{\partial T(L)}{\partial Z} = 0$
$C_t(0) = \frac{P(0)}{RT(0)}$ where $P(0) = P^{in} \succ P_{AD}$	$P(L) = P_{AD}$
Depressurization pressure equalization (DPE)	
$u(0) = 0$	$\frac{\partial C_j(L)}{\partial Z} = 0$
$\frac{\partial T(0)}{\partial Z} = 0$	$\frac{\partial T(L)}{\partial Z} = 0$
$\frac{\partial C_j(0)}{\partial Z} = 0$	$C_t(L) = \frac{P(L)}{RT(L)}$ where $P(L) = P_{PE} + (P_{AD} - P_{PE})\exp(-Kt)$
Blowdown (BD)	
$\frac{\partial C_j(0)}{\partial Z} = 0$	$u(L) = 0$
$\frac{\partial T(0)}{\partial Z} = 0$	$\frac{\partial T(L)}{\partial Z} = 0$
$C_t(0) = \frac{P(0)}{RT(0)}$ where $P(0) = P_{AD}$	$\frac{\partial C_j(L)}{\partial Z} = 0$
Purge (PG)	
$\frac{\partial C_j(0)}{\partial Z} = 0$	$-\xi_b D_Z \frac{\partial C_j(L)}{\partial Z} = u(L)(C_j^{in} - C_j(L))$
$\frac{\partial T(0)}{\partial Z} = 0$	$-\xi_b K_Z \frac{\partial T(L)}{\partial Z} = \rho_g(L)C_{pg}(L)u(L)(T^{in} - T(L))$
$P(0) = P_{PG}$	$C_t(L) = \frac{P(L)}{RT(L)}$ where $P(L) = P^{in} \succ P_{PG}$
Pressurization pressure equalization (PPE)	
$u(0) = 0$	$-\xi_b D_Z \frac{\partial C_j(L)}{\partial Z} = u(L)(C_j^{in} - C_j(L))$
$\frac{\partial T(0)}{\partial Z} = 0$	$-\xi_b K_Z \frac{\partial T(L)}{\partial Z} = \rho_g(L)C_{pg}(L)u(L)(T^{in} - T(L))$
$\frac{\partial C_j(0)}{\partial Z} = 0$	$C_t(L) = \frac{P(L)}{RT(L)}$ where $P(L) = P_{PE} + (P_{PG} - P_{PE})\exp(-Kt)$
Pressurization (PR)	

$-\xi_b D_Z \frac{\partial C_j(0)}{\partial Z} = u(0)(C_j^{Feed} - C_j(0))$	$u(L) = 0$
$-\xi_b K_Z \frac{\partial T(0)}{\partial Z} = \rho_g(0) C_{pg}(0) u(0)(T^{Feed} - T(0))$	$\frac{\partial T(L)}{\partial Z} = 0$
$C_t(0) = \frac{P(0)}{RT(0)}$	$\frac{\partial C_j(L)}{\partial Z} = 0$
where $P(0) = P_{PE} + (P_{PR} - P_{PE}) \exp(-Kt)$	

Table 4: Boundary conditions for each step in the PSA simulation.

The dynamic adsorption bed and the PSA simulation are carried out using **Aspen Adsorption** software**.**

IV. RESULTS AND DISCUSSION

IV.1 Adsorption equilibria

Single-component adsorption isotherms of CO2, CO, CH4, and H2 on commercial activated carbon were measured at different temperatures 30, 40, and 50 °C using fresh adsorbent. The adsorption equilibrium of multi-component model was predicted by dual-site Langmuir model based on monocomponent experimental isotherms data. The adsorption equilibrium isotherms for CH_4, CO, CO_2 and H_2 on commercial activated carbon are plotted in Figures 4 to 7. Dual-site Langmuir parameters, heats of adsorption and linear driving force parameters are summarized in Table 5.

	H_2	*CH_4*	*CO_2*	*CO*
K_1[mol/kg.bar]	*$2.17.(10^{-7})$*	*$2.90.(10^{-7})$*	*$6.54.(10^{-9})$*	*$1.93.(10^{-7})$*
K_2[K]	*1260*	*2370*	*3620*	*2160*
K_3[1/bar]	*$9.24.(10^{-5})$*	*$8.71.(10^{-5})$*	*$1.12(10^{-6})$*	*$1.64.(10^{-4})$*
K_4[mol/kg.bar]]	*$2.17.(10^{-7})$*	*$3.60.(10^{-7})$*	*$2.92.(10^{-8})$*	*$1.93.(10^{-7})$*
K_5[1/bar]	*$9.24.(10^{-5})$*	*$7.96.(10^{-4})$*	*$2.0.(10^{-5})$*	*$1.64.(10^{-4})$*
k [1/s]	*4*	*4*	*4*	*4*
ΔH_{ads}[J/mol]	*10494*	*19678.76*	*30100*	*17968*

Table 5: Dual-site Langmuir parameters, heats of adsorption and linear driving force parameters of gases on a commercial activated carbon.

The isotherms of CO and CO2 were of irreversible type in the low-pressure range. The local adsorption rate of CO, CO2 on adsorbent are considered to be fast enough to assume instantaneous equilibrium.

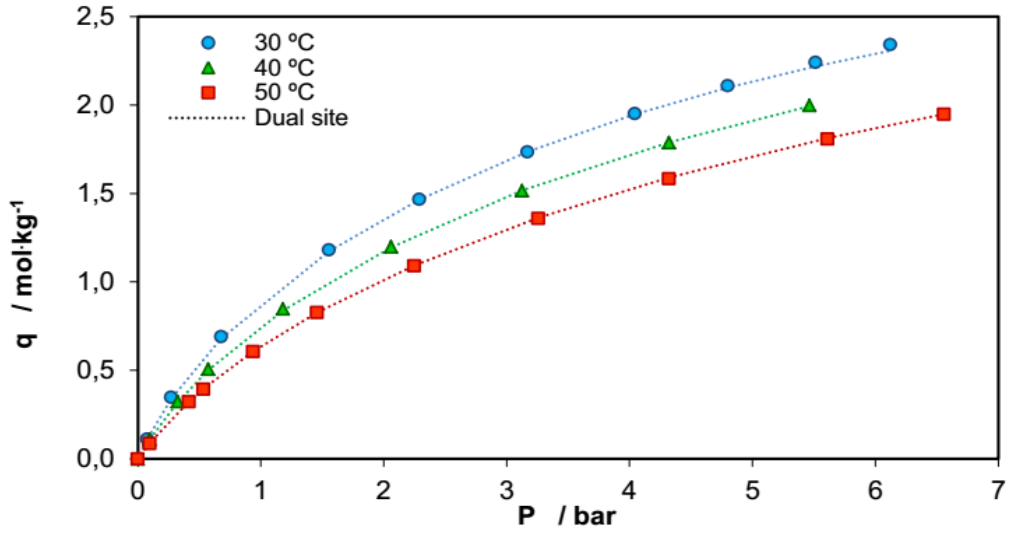

Figure 4: CH4 isotherms at different temperatures on commercial activated carbon.

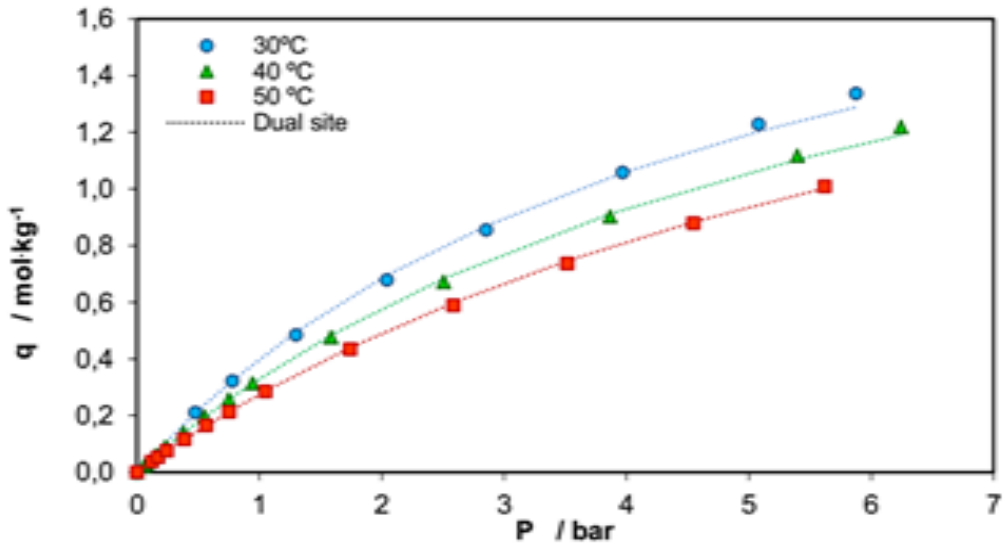

Figure 5: CO isotherms at different temperatures on commercial activated carbon.

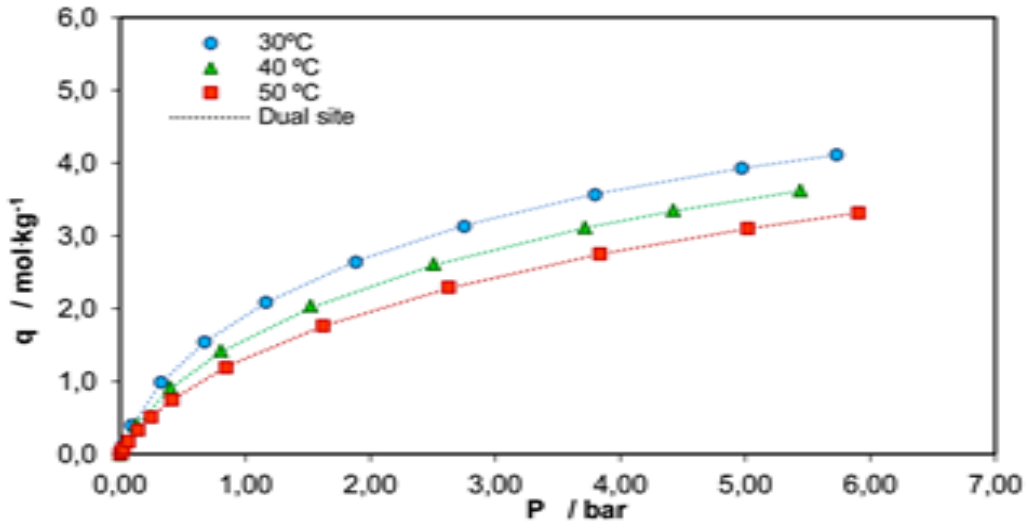

Figure 6: CO_2 isotherms at different temperatures on commercial activated carbon.

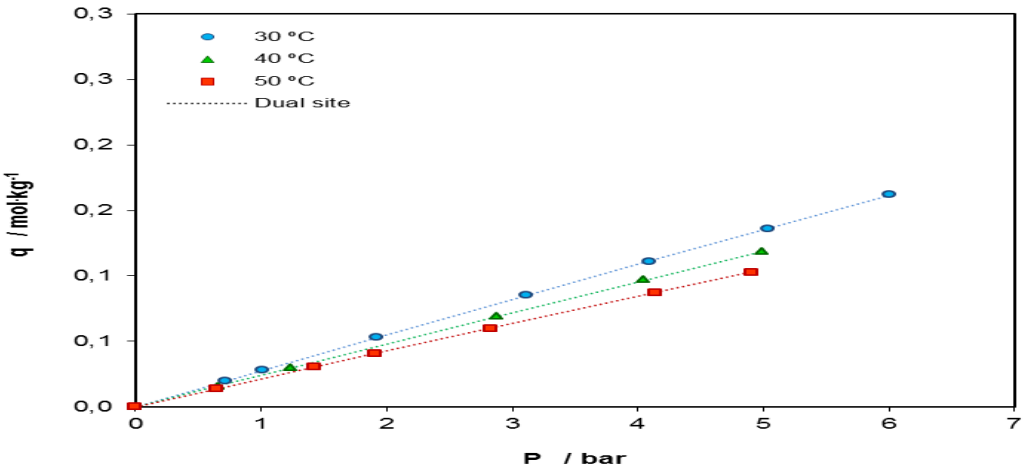

Figure 7: H_2 isotherms at different temperatures on commercial activated carbon.

IV.2 Breakthrough dynamics of the adsorption bed

IV.2.1 Concentration profile

A hydrogen mixture (CO:CO2:CH4:H2:He = 1:25:5:20:49 mol.%) was fed to an adsorption bed containing a commercial activated carbon. The breakthrough experiment was carried out at 40 °C, 1 bar and using a feed flow rate of 0.5 L/min. The bed was initially filled with pure helium.

The comparison of the simulation results with the experimental data is reported in figure 8.

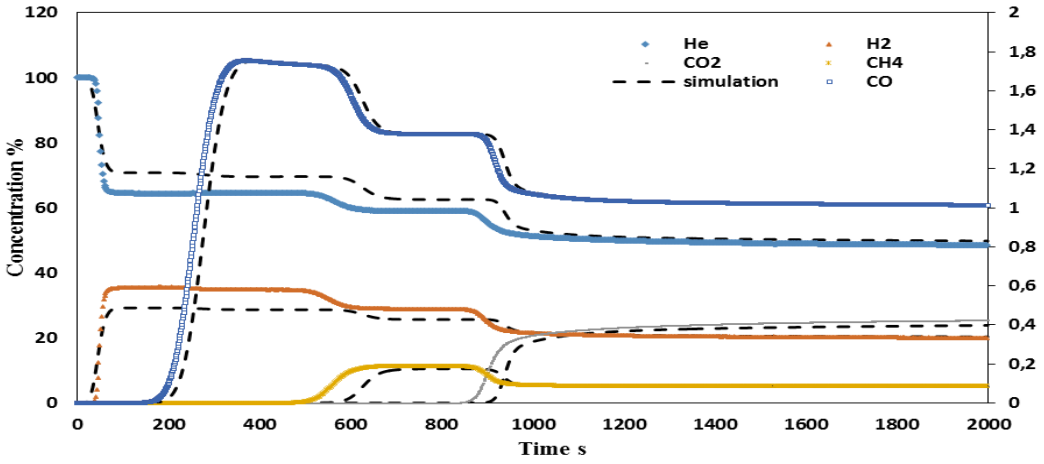

Figure 8: Comparison between the simulation results and the experimental breakthrough data.

H2 adsorbs only slightly. The first contaminant to break through the column is carbon monoxide, followed by methane and finally by carbon dioxide.

IV.2.2 Temperature profile

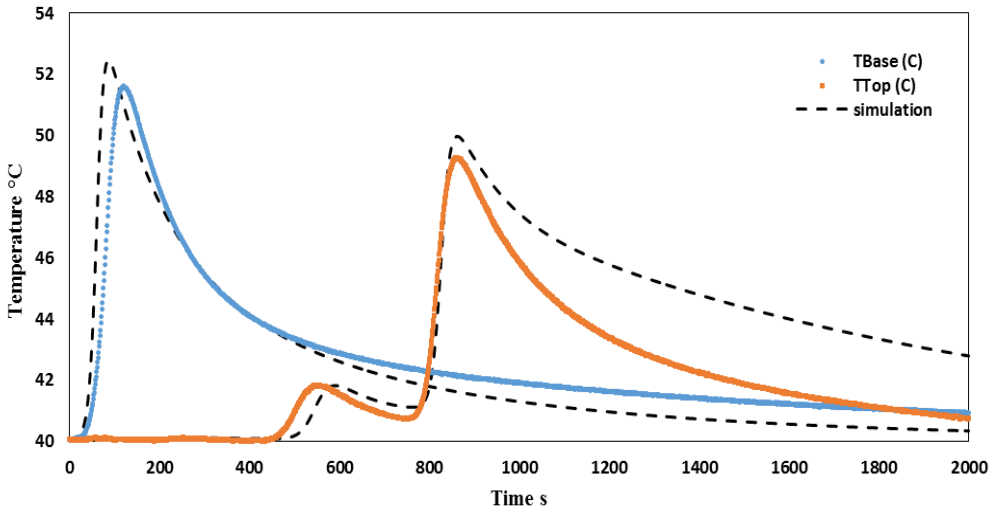

Figure 9: Temperature evolution with time at the top and the bottom of the column.

The temperature evolution is given in figure 9.

At the exit of the column, the two peaks of temperature appearing at nearly 600 and 1000 s correspond to the adsorption heat generated by moving concentration fronts of CH4 and CO2 respectively. Due to the low amount of H2 adsorbed and the low concentration of CO in the feed mixture, the temperature peaks corresponding to these components are not detected. The temperature evolution just after the bed inlet displays only one peak corresponding to all components of the mixture; the reason is that at this axial position, concentration waves of the different components are not yet separated, thus leading to the formation of only one temperature front. Once saturated, the packed bed temperature decreases gradually due to heat transfer with both gas mixture and column-wall.

The dynamic mathematical model could predict the experimental temperature profiles along the bed length reasonably well.

IV.3 Pressure Swing Adsorption process

After confirmation of the validity of multicomponent adsorption equilibrium and kinetic data, a PSA experiment was performed to validate the mathematical model in a cyclic experiment.

A four-column PSA experiment was performed using cycle scheduling illustrated in Figure 4.The experimental run was performed at ambient temperature at a feed flow rate of 1.37 L/min and the following composition: 74% of H2, 25% of CO2, 1% of CH4 and 1% of CO. The pressure feed was fixed at 8.5 bars and the blowdown pressure was 1 bar. The experimental conditions are shown in table 6.

Operating conditions	
Adsorption pressure, [bar]	8.5
Desorption pressure, [bar]	1
Feed temperature,[°C]	24.6
Feed flow rate,[L/min]	1.37
Purge flow rate ,[L/min]	0.2
Production flow rate,[L/min]	0.75

Table 6: Operating conditions.

The pressure history for one cycle is shown in Figure 10. The molar flow rate histories obtained for four cycles are reported in Figure 11, 12 and 13.

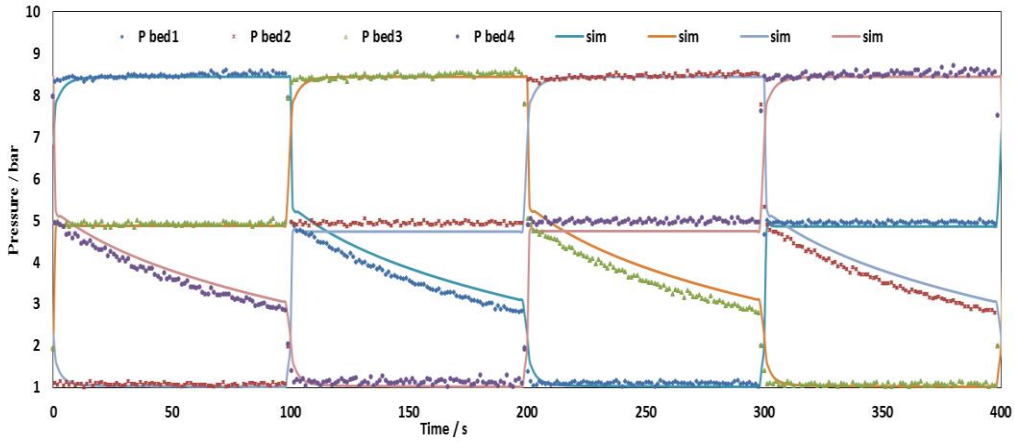

Figure 10: Pressure history of four-column for one cycle

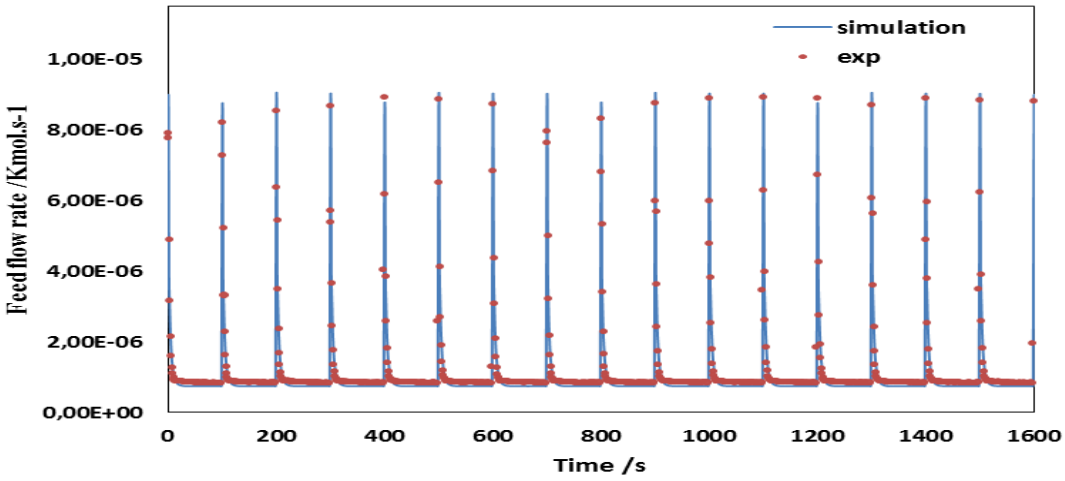

Figure 11: Feed flow rate profiles for four cycles after the steady state.

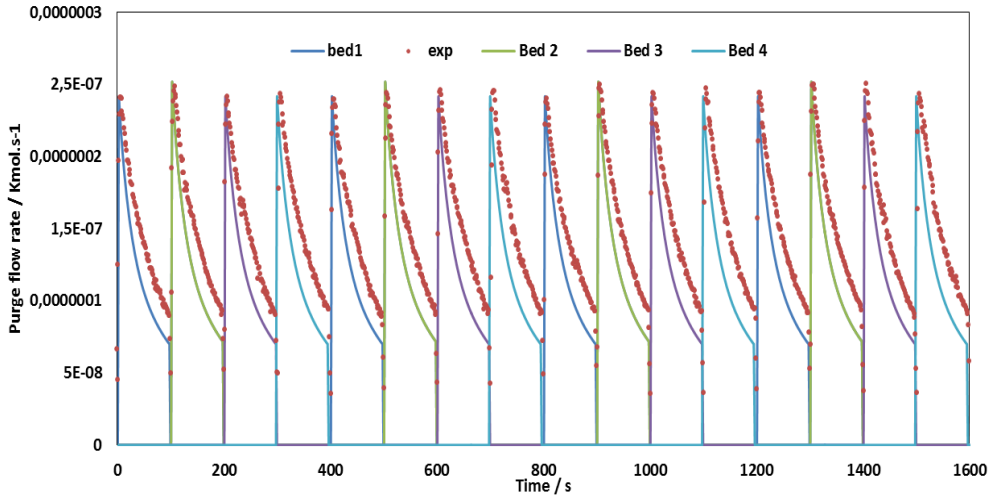

Figure 12: Purge flow rate profiles for four cycles.

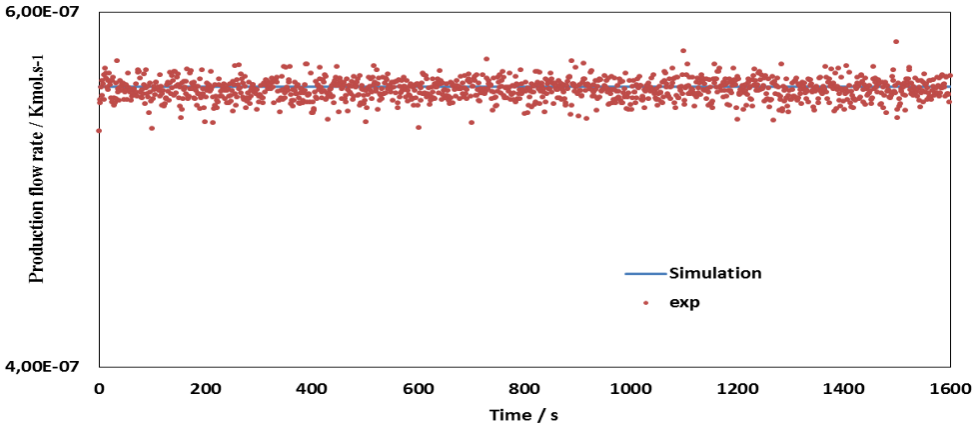

Figure 13: Production flow rate for four cycles.

In these four cycles, a good agreement between simulation and the experimental molar flow rates was observed.

In the PSA simulation a 99.9913 % hydrogen purity stream (with 84.39 ppm of CO, 0.17 ppm of CO2 and 0.9 ppm of CH4 contamination) was obtained with a hydrogen recovery of 75.5 %.

V. CONCLUSION

A rigorous mathematical model that includes mass, energy and momentum balances was employed to elucidate the dynamic behaviours and separation performance of the adsorption bed. A valid parameter set has been obtained from adsorption isotherms and breakthrough experiments. Good agreement between simulation results and the experimental data was achieved for both breakthrough curves and temperature profiles.

Future work will focus on optimization of the process to reach a CO concentration between 10 and 20 and recovery greater or equal to 75 %.

REFERENCES

[1] Hord J. Hydrogen safety: an annotated bibliography of regulations, standards and guidelines. *Int J HydrogEnergy* 1980:579–84.

[2] Das D, Veziroglu TN. Advances in biological hydrogen production processes.*Int J Hydrog Energy* 2008; 33(21):6046–57.

[3] Malek A, Farooq S. Hydrogen purification from refinery fuel gas by pressure swing adsorption. *AIChE Journal* 44. 1998, 1985–1992.

[4] Ribeiro AM, Grande CA, Lopes FVS, Loureiro JM, Rodrigues AE. Chem Eng Sci 2008; 63:5258–73.

[5] Lee, J.-J., Kim, M.-K., Lee.D.-G., Ahn,H. , Kim,M.J.Lee, C-H, 2008 Heat-exchange pressure swing adsorption process for hydrogen separation.*AICHE Journal* 54, 2054-2064.

[6] Ritter, J.A., Yang, R.T., 1987.Equilibrium adsorption of multicomponent gas mixtures at elevated pressures. *Industrial and Engineering ChemistryResearch* 26, 1679-1686.

[7] Santos, J. C.; Magalhaes, F. D.; Mendes, A. Contamination of Zeolites Used in Oxygen Production by PSA: Effects of Water and Carbon Dioxide. *Ind. Eng. Chem. Res*. 2008, 47 (16), 6197–6203.

[8] Ferreira. D, Magalhaes.R, Taveira.P and Mendes, A.Effective Adsorption Equilibrium Isotherms and Breakthroughs of Water Vapor and Carbon Dioxide on Different Adsorbents. *Ind. Eng. Chem.Res*.2011, 10201-1021.

[9] Mauro Luberti, Daniel Friedrich, Stefano Brandani , Hyungwoong Ahn, Design of a H2 PSA for cogeneration of ultrapure hydrogen and power at an advanced integrated gasification combined cycle with pre-combustion capture. *Adsorption* 2014 20:511–524.